Interplay of Intrinsic and Environmental Effects on the Magnetic Properties of Free Radicals Issuing from H-Atom Addition to Cytosine

Carlo Adamo,[†] Marie Heitzmann,[‡] Flora Meilleur,[‡] Nadia Rega,[†] Giovanni Scalmani,[†] Andre Grand,[‡] Jean Cadet,[‡] and Vincenzo Barone*,[†]

Contribution from the Dipartimento di Chimica, Complesso Universitario di Monte S. Angelo, via Cintia, I-80126 Napoli, Italy, Laboratoire de Lesions des Acides Nucleiques, Service de Chimie Inorganique et Biologique, Dèpartment de Recherche Fondamentale sur la Matière Condensée and UMR 5046, CEA-Grenoble, F-38054 Grenoble, Cedex 09, France

Received December 18, 2000

Abstract: Possible radical reaction products issuing from H-atom addition to cytosine have been characterized and analyzed by means of a comprehensive quantum mechanical approach including density functional computations (B3LYP), together with simulation of the solvent by the polarizable continuum model (PCM), and averaging of spectroscopic properties over the most important vibrational motions. The hyperfine couplings of the semirigid 5,6-dihydrocytos-6yl radical computed at the optimized geometry are in good agreement with their experimental counterparts. On the other hand, vibrational averaging is mandatory for obtaining an effectively planar structure for the 5,6-dihydrocytos-5yl radical with the consequent equivalence of β-hydrogens. Finally, only proper consideration of environmental effects restores the agreement between computed and experimental couplings for the base anion protonated at N3.

Introduction

The radicals originated by radiation damage to nucleic acids initiate chemical reactions that are responsible for DNA alterations, including strand breaks and base modifications. These radicals result either from the direct ionization of the DNA bases or from reactions with hydrated electrons or with species issuing from water radiolysis, namely hydrogen ($H^{\bullet}$) and hydroxyl ($OH^{\bullet}$) radicals. Evidence is accumulating that when the attack occurs at pyrimidine bases, the predominant reaction is an addition to double bonds, whereas the main mode of attack on the sugar phosphate backbone is hydrogen abstraction.[1−3] Furthermore, solvated electrons can add to the DNA bases to form anion radicals; irreversible protonation of the latter radicals at a carbon atom produces the same species issuing from direct H addition to the base.[4] For instance, addition of a H atom to the C5−C6 bond of thymine or cytosine bases leads to the formation of different stable products with a saturated C5−C6 bond. Alternatively, the attack of the H atom can lead to a base anion protonated at N3. Still, however, relatively little detailed knowledge exists regarding the reaction mechanism and, to some extent, the form (neutral, charged) in which the radicals are generated. The identification of these radical species is generally attempted using electron paramagnetic resonance (EPR) spectroscopy.[5−11] Although this spectroscopy provides a direct experimental measure of the distribution of the unpaired spin density,[12,13] only partial information is available, usually concerning the hyperfine coupling constants (hcc's) of hydrogen atoms.

In such circumstances, quantum mechanical approaches can provide a valuable support to the experiment, especially when either concurrent interpretations are possible or detailed structure/observable relationships are needed. A further interest in theoretical methods rests on the easy evaluation of the contribution of various terms to the overall result, which can be finely tuned by switching different interactions on or off in the computations. Obviously, the computational protocol must provide reliable structural and magnetic properties, in particular for large systems that are of current chemical and biological interest.

In recent years, it has been shown that hybrid Kohn−Sham/Hartree−Fock (KS/HF) methods are quite promising in this respect when coupled to a proper treatment of averaging effects issuing from large-amplitude vibrations.[14−16] More recently, this

* Corresponding author. E-mail: Enzo@lsdm.dichi.unina.it.
[†] Università "Federico II".
[‡] CEA-Grenoble.

(1) Weitzman, S. A.; Turk, P. W.; Milkowski, D. H.; Kozlowski, K. *Proc. Natl. Acad. Sci. U.S.A.* **1994**, *91*, 1261.
(2) Steenken, S. *Chem. Rev.* **1989**, *89*, 503.
(3) von Sonntag, C. *Chemical Basis of Radiation Biology*; Taylor and Francis: London, 1987.
(4) Becker, D.; Sevilla, M. D. In *Advances in Radiation Biology*; Lett, J., Ed.; Academic Press: New York, 1993, Vol. 17.
(5) Pershan, P. S.; Shulman, R. G.; Wyluda, B. J.; Eisinger, J. *Science* **1965**, *148*, 378.
(6) Flossmann, W.; Westhof, E.; Müller, A. *Int. J. Radiat. Biol.* **1976**, *30*, 301.
(7) (a)Westhof, E. *Int. J. Radiat. Biol.* **1973**, *23*, 389. (b) Westhof, E.; Lion, Y.; van de Vorst, A. *Int. J. Radiat. Biol.* **1977**, *32*, 499.
(8) Close, D. M.; Sagstuen, E. *J. Chem. Phys.* **1983**, *79*, 5292.
(9) Sagstuen, E.; Hole, E.; Nelson, W. H.; Close, D. M. *J. Phys. Chem.* **1992**, *92*, 8269.
(10) Barnes, J. P.; Berhnard, W. A. *J. Phys. Chem.* **1994**, *98*, 887.
(11) Hole, E. O.; Nelson, W. H.; Sagstuen, E.; Close, D. M. *Radiat. Res.* **1998**, *149*, 109.
(12) Fermi, E. *Z. Physik*, **1930**, *60*, 320.
(13) Abragam, A.; Pryce, M. H. L. *Proc. R. Soc. A* **1951**, *205*, 135.
(14) Barone, V. *Theor. Chim. Acta* **1995**, *91*, 113.
(15) Barone, V. In *Recent Advances in Density Functional Methods, Part 1*; Chong, D. P., Ed.; World Scientific Publishing Co.: Singapore, 1996.
(16) Barone, V.; Adamo, C.; Brunel, Y.; Subra, R. *J. Chem. Phys.* **1996**, *105*, 3168.

10.1021/ja004284z CCC: $20.00
Published on Web 06/30/2001

computational approach has been extended to condensed phases,[17,18] adding to the above features the effect of a polarizable continuum mimicking the solvent. Because the results of this protocol are very promising,[19,20] we decided to study the structure, harmonic frequencies, and EPR features of three of the major products arising from the addition of an H atom to cytosine, namely, the 5,6-dihydrocytos-5-yl (hereafter, 5-yl) and the 5,6-dihydrocytos-6-yl (hereafter, 6-yl) radicals and the base anion that is protonated at N3 (hereafter, N3H). In the case of the 5-yl and 6-yl radicals, a wide set of hyperfine coupling constants is available for the methylene group at positions 6 and 5, even if the experimental conditions are very different, ranging from frozen aqueous solution[7] to monocrystals.[6,8,9] In all cases, the two β protons exhibit equal hyperfine coupling constants. In addition, the hyperfine coupling constant of H^{α} and H^{β} atoms are not always unambiguously defined because of the weakness of the signal.[9] Only a few data are available for the N3H radical, for which three different couplings have been assigned.[9] Previous quantum mechanical computations[21] dealt only partially with the structure assignment of the latter radicals; moreover, they did not resolve the puzzling problems posed by the interpretation of the EPR spectra and by the structure/observable relationships.[22,23]

In such a context, a deeper computational study aimed at rationalizing the structural effects on the observed hyperfine coupling constants should provide valuable information for the experimentalists.

Computational Details

All of the electronic calculations were carried out with the Gaussian 98 code[24] using the B3LYP computational model,[25−28] which has been tested and validated in a number of studies on organic radicals.[15,29,30]

The 6-31G(d) and 6-311G(d,p) basis sets[31] were our standards for all of the geometry optimizations; using these structures, improved magnetic properties were obtained by the EPR-II and EPR-III basis sets,[31] which were specifically optimized for computing isotropic hyperfine coupling constants.[15]

The isotropic hyperfine coupling constants, a_N, are related to the spin densities at the corresponding nuclei by[32]

$$a_N = \frac{8\pi}{3h} g_e \beta_e g_N \beta_N \sum_{\mu,\nu} P^{\alpha-\beta}_{\mu,\nu} \langle \varphi_\mu | \delta(r_{kN}) | \varphi_\nu \rangle$$

where β_e and β_N are the electron and nuclear magneton, respectively; g_e and g_N are the corresponding magnetogyric ratios; h, the Planck constant; δ(r) is a Dirac delta operator; and $P^{\alpha-\beta}$ is the difference between the density matrices for electrons with α and β spins. In the present work, all of the values are given in Gauss (1 G = 0.1 mT), assuming that the free electron g value is appropriate also for the radicals. To convert data to MHz, one has to multiply them by 2.8025.

For large systems, any effective treatment of vibrational averaging effects rests on some separation between a small number (in most cases, one) of active large amplitude motions (LAMs) and the spectator small amplitude modes (SAMs). In the present work, the LAM is assumed to occur along the linear synchronous path (LSP)[33] connecting pairs of related energy minimums, which is invariant upon isotopic substitution and well-defined also beyond energy minimums. Then the path in mass-weighted coordinates is parametrized in terms of its arc length, s, referred to as the linear synchronous coordinate (LSC). When the couplings connecting SAMs among themselves and with the LSC are negligible, we end up with an effective one-dimensional Hamiltonian governing motion along the LSP, whose eigenvalues can be found using the numerical procedure described elsewhere.[15,34] Then, the expectation value $\langle O \rangle_T$ of a given observable at absolute temperature T is given by

$$\langle O \rangle_T = O_{ref} + \frac{\sum_{j=0}^{\infty} \langle j|\Delta O|j\rangle \exp[(\epsilon_0 - \epsilon_j)/KT]}{\sum_{j=0}^{\infty} \exp[(\epsilon_0 - \epsilon_j)/KT]}$$

where O_{ref} is the value of the observable for the reference structure (in the present context, the absolute energy minimum), $\Delta O(s)$ is the expression (here, a spline fit) giving its variation as a function of the progress variable s, and $|j>$ is a vibrational eigenstate with eigenvalue ϵ_j. All of these computations were performed using the DiNa program developed by one of us.[34]

Solvent effects were evaluated using a recent implementation of the polarizable continuum model (PCM) in the Gaussian package.[35,36] In particular, optimized structures and solvation energies have been computed by an optimized cavity model, namely the united atom topological model (UATM),[37] coupled to the conductor-like polarizable continuum model (CPCM).[38] The details of this procedure have been extensively described elsewhere.[37,38] Here, we simply recall that this approach provides results very close to those obtained by the original dielectric model for high-dielectric-constant solvents, but it is significantly more effective in geometry optimizations, and less prone to numerical errors arising from the small part of the solute electron cloud lying outside the cavity (escaped charge effects).[38]

(17) Rega, N.; Cossi, M.; Barone, V. *J. Chem. Phys.* **1996**, *105*, 11060.
(18) Rega, N.; Cossi, M.; Barone, V. *J. Am. Chem. Soc.* **1997**, *119*, 12962; **1998**, *120*, 5723.
(19) Barone, V.; Bencini, A.; di Matteo, A. *J. Am. Chem. Soc.* **1997**, *119*, 10831.
(20) Barone, V.; Bencini, A.; Cossi, M.; di Matteo, A.; Mattesini, M.; Totti, F. *J. Am. Chem. Soc.* **1998**, *120*, 7069. Barone, V.; Bencini, A.; Ciofini, I.; Daul, C. *J. Phys. Chem. A* **1999**, *103*, 4275. Nielsen, P. A.; Norrby, P. O.; Liljefors, T.; Rega, N.; Barone, V. *J. Am. Chem. Soc.* **2000**, *122*, 3151. Improta, R.; di Matteo, A.; Barone, V. *Theor. Chem. Acc.* **2000**, *104*, 273.
(21) Wetmore, S. J.; Himo, F.; Boyd, R. J.; Eriksson, L. A. *J. Phys. Chem. B* **1998**, *102*, 7484.
(22) Close, D. M.; Sagstuen, E.; Hole, E. O.; Nelson, W. H. *J. Phys. Chem. B* **1999**, *103*, 3049.
(23) Wetmore, S. J.; Boyd, R. J.; Himo, F.; Eriksson, L. A. *J. Phys. Chem. B* **1999**, *103*, 3051.
(24) Frisch, M. J.; Trucks, G. W.; Schlegel, H. B.; Scuseria, G. E.; Stratmann, R. E.; Burant, J. C.; Dapprich, S.; Millam, J. M.; Daniels, A. D.; Kudin, K. N.; Strain, M. C.; Farkas, O.; Tomasi, J.; Barone, V.; Cossi, M.; Cammi, R.; Mennucci, B.; Pomelli, C.; Adamo, C.; Clifford, S.; Ochterschi, J.; Cui, Q.; Gill, P. M. W.; Johnson, B. G.; Robb, M. A.; Cheeseman, J. R.; Keith, T.; Petersson, G. A.; Morokuma, K.; Malick, D. K.; Rabuck, A. D.; Montgomery, J. A.; Raghavachari, K.; Al-Laham, M. A.; Zakrewski, V. G.; Ortiz, J. V.; Foresman, J. B.; Cioslowski, J.; Stefanov, B. B.; Nanayakkara, A.; Liu, J.; Liashenklo, A.; Piskorz, P.; Komaromi, I.; Challacombe, M.; Peng, C. Y.; Ayala, P. Y.; Chen, W.; Wong, M. W.; Andres, J. L.; Replogle, E. S.; Gomperts, R.; Martin, R. L.; Fox, D. J.; Binkley, J. S.; DeFrees, D. J.; Baker, J.; Stewart, J. P.; Head-Gordon, M.; Gonzalez, C.; Pople. J. A. *Gaussian 98 (Revision A.7)*; Gaussian, Inc.: Pittsburgh, PA, 1999.
(25) Becke, A. D. *J. Chem. Phys.* **1993**, *98*, 1372.
(26) Becke, A. D. *Phys. Rev. B* **1988**, *38*, 3098.
(27) Lee, C.; Yang, W.; Parr, R. G. *Phys. Rev. B* **1988**, *37*, 785.
(28) Becke, A. D. *J. Chem. Phys.* **1993**, *98*, 5648.
(29) Adamo, C.; Barone, V.; Fortunelli, A. *J. Chem. Phys.* **1995**, *102*, 384.
(30) Adamo, C.; Subra, R.; di Matteo, A.; Barone, V. *J. Chem. Phys.* **1998**, *109*, 10224.
(31) Frisch, Æ.; Frisch, M. J. *Gaussian 98 User's Reference*; Gaussian, Inc.: Pittsburgh, 1998.
(32) Weltner, W., Jr. *Magnetic Atoms and Molecules*; Dover: New York, 1989.
(33) Halgren, T. A.; Lipscomb, W. N. *Chem. Phys. Lett.* **1977**, *49*, 225.
(34) Barone, V. *J. Phys. Chem.* **1995**, *99*, 11659. Minichino, C.; Barone, V. *J. Chem. Phys.* **1994**, *100*, 3717.
(35) Cossi, M.; Barone, V.; Cammi, R.; Tomasi, J. *Chem. Phys. Lett.* **1996**, *255*, 327.
(36) Barone, V.; Cossi, M.; Tomasi, J. *J. Chem. Phys.* **1997**, *107*, 3210.
(37) Barone, V.; Cossi, M.; Tomasi, J. *J. Comput. Chem.* **1998**, *19*, 407.
(38) Barone, V.; Cossi, M. *J. Phys. Chem. A* **1998**, *102*, 1995.

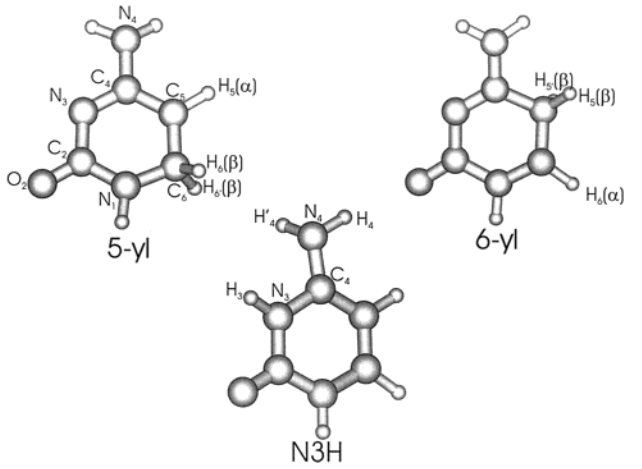

Figure 1. Structure and atom numbering of 5-yl, 6-yl, and N3H radicals.

Results and Discussion

The structural features of cytosine have already been discussed extensively (see, for instance, refs 39−43) and will not be discussed in depth here. We point out only that the B3LYP and MP2[40] geometries are very close, thus confirming that the B3LYP method is efficient and reliable for structural analyses of closed-shell systems. Furthermore, the B3LYP results are not significantly dependent on the basis set, 6-31G(d) and 6-311G(d,p) results being very close.

Several detailed studies dealt with the vibrational spectrum of cytosine (see for instance, refs 40, 44, and 45), some of them showing the reliability of the B3LYP/6-31G(d) model.[40,45] Because our computations do not differ from those already reported, either in the computed values or in the assignment, we refer the reader to these papers for detailed analysis of the cytosine IR spectrum.[40,46] Even if the quality of the B3LYP/6-31G(d) spectrum is quite good, scaling all of the frequencies with a single factor (0.956)[47] significantly improves the agreement with experiments. As a consequence, we used the same factor to scale the frequencies of the radicals considered in the present study (see Figure 1).[48]

In agreement with a previous DFT study,[21] in vacuo the energetically most stable radical species is N3H, whereas 5-yl and 6-yl radicals are 7−8 kcal/mol less stable; however, in aqueous solution, the three radicals have a comparable stability, because the N3 atom (present in 5-yl and 6-yl) is much better solvated (via its lone pair) than the NH group present in N3H. Other possible neutral species are significantly less stable and will not be considered in the following.

The geometry of cytosine changes significantly upon H atom attack. In particular, an increase of about 0.13 Å is found for the C5C6 bond in both 6-yl and 5-yl radicals: this is expected for the conversion of a double into a single bond. Significant variations are also found for the N1C6 bond in the 5-yl radical and for the C4C5 bond in the 6-yl species. A different pattern is found for the N3H radical, because the addition of a H atom to the N3 position induces the largest variation on the N3C4 bond (+0.09 Å) and, as a consequence of the breaking of the bonding pattern, on C4C5 (+0.06 Å) and C5C6 (−0.06 Å) bonds. The most noticeable feature is, anyway, the nonplanarity of the NH_2 group, the N4 atom showing an sp^3-like hybridization (the $H_4N_4H_4'$ valence angle is 109.5°), with one hydrogen atom significantly out of the molecular plane (see Figure 1).

In all of the radicals, the six-membered ring is more or less significantly puckered (see Figure 1 and Table 1). In particular, the six-membered ring is nearly planar for the 5-yl radical, whereas it is more significantly distorted in the 6-yl and N3H radicals.

For all of the radicals, the planar structure is a first-order saddle point, less stable than the energy minimum by 18 kJ/mol for N3H, by 2 kJ/mol for 6-yl, and by only 0.8 kJ/mol for 5-yl at the B3LYP/6-311G(d,p) level.

The experimental data available for the isotropic hcc's of the different radicals under different conditions are summarized in Table 2, and our computed values are compared in Table 3 with previous results obtained using similar geometries but a different density functional.[21] Although both sets of results are quite similar, our values are generally slightly larger. The authors of ref 21 concluded that the deviation from the observed hyperfine couplings could be ascribed to an insufficient ring puckering issuing from DFT computations. Here, we analyze other effects, which can lead the computed values to be in better agreement with their experimental counterparts.

Let us begin our analysis with the 5-yl radical. The experimental data suggest two equivalent hydrogens, with a coupling ranging between 48.8 and 55 G, depending upon the experimental conditions. The B3LYP/EPRII values for the two H^{β} atoms computed at the equilibrium geometry are very close (51.3 and 50.1 G, respectively) and are only slightly modified by extension of the basis set and by inclusion of environmental effects by the PCM. Although vibrational averaging does not introduce huge modifications, it leads the computed value into better agreement with experiment (52.1 vs 55 G) and, especially, makes the H^{β} atoms strictly equivalent. A good agreement is found also for the hcc of H^{α}, whose best theoretical estimate (−18.5 G) is close to the experimental value in frozen aqueous solution (±16.7 G)[7a] and nearly identical to the most recent ENDOR determination (−18.4 G).[9]

Also for the 6-yl radical, the hcc of the H^{α} atom is well reproduced by our computations. The situation is more involved for the β protons, which are placed asymmetrically with respect to the ring plane and display two strongly nonequivalent hcc's in the equilibrium structure (48.0 and 15.0 G, respectively, at the B3LYP/EPR-II level). On the other hand, the experimental value is 40.0 G at 77,K for both hydrogens, which is quite close to the value computed for the planar form (38.0 G), in which both H^{β}'s are, of course, equivalent. Extension of the basis set and inclusion of environmental effects by the PCM do not change the results in a significant way (see Tables 3 and 4).

This situation calls for an adequate treatment of the effects of the inversion motion on the chemical observable; therefore, we have analyzed in further detail the energy profile along the LSP governing the inversion of the half-chair structure of 6-yl. The potential curve governing inversion at the radical center shows two relatively deep minimums corresponding to the two symmetric half-chair conformations (see Figure 2), and the

(39) Taylor, R.; Kennard, O. *J. Mol. Struct*. **1982**, *78*, 1.
(40) Aamouche, A.; Ghomi, M.; Grajcar, L.; Baron, M. H.; Romain, F.; Baumruk, V.; Stepanek, J.; Coulombeau, C.; Jobic, H.; Berthier, G. *J. Phys. Chem. A* **1997**, *101*, 10063.
(41) Kobayashi, R. *J. Phys. Chem. A* **1998**, *102*, 10813.
(42) Fogarasi, G. *J. Mol. Struct*. **1997**, *413*, 271.
(43) Les, A.; Adamowicz, L.; Bartlett, R. *J. Phys. Chem*. **1989**, *93*, 4001.
(44) Florián, J.; Baumruk, V.; Leszczynski, J. *J. Phys. Chem*. **1996**, *100*, 5578.
(45) Kwiatkowski, J. S.; Leszczynski, J. *J. Phys. Chem*. **1996**, *100*, 941.
(46) Szczesniak, M.; Szczczepaniak, K.; Kwiatkowski, J. S.; Kubulat, K.; Person, W. *J. Am. Chem. Soc.* **1988**, *110*, 8319.
(47) Rauhut, G.; Pulay, P. *J. Phys. Chem*. **1995**, *99*, 3093.
(48) Jolibois, F.; Cadet, J.; Grand, A.; Rega, N.; Subra, R.; Barone, V. *J. Am. Chem. Soc*. **1998**, *120*, 1864.

Table 1. Selected Dihedral Angles (degrees) of the Considered Radicals, Computed at the UB3LYP Level

	N3H		6-yl		5-yl	
	6-31G(d)	6-311G(d,p)	6-31G(d)	6-311G(d,p)	6-31G(d)	6-311G(d,p)
C5−C4−N3−C2	6.2	5.3	4.5	4.1	2.3	1.8
N1−C2−N3−C4	−8.2	−6.6	8.8	9.9	1.3	−0.8
C6−N1−C2−N3	6.9	5.5	0.8	−0.5	−7.8	−2.0
O7−C2−N1−C6	−173.5	−174.5	−178.1	−171.6	172.8	177.9
H4−N4−C4−C5	118.0	119.4	171.3	173.8	168.0	169.0
H4′-N4−C4−C5	−5.1	−5.5	11.6	6.3	27.8	25.0
N3−C4−C5−H5	176.9	177.0	−146.6	−147.1	179.5	179.7
N3−C4−C5−H5′			98.3	97.7		
C2−N1−C6−H6	177.2	117.6	−177.3	−178.5	131.1	125.1
C2−N1−C6−H6′					−112.7	−118.6

Table 2. Experimental Hyperfine Coupling (G) Constants for the Considered Cytosyl Radicals

source	H_α	$H_{\beta1}$	$H_{\beta2}$	experimental condition
			6-yl	
ref 7b	±18.6	±40	±40	frozen aqueous solution 77 K
ref 7a	±18.6	±37.5	±37.5	crystal, 298 K
ref 9	−18.7 (1)			crystal, 10 K
			5-yl	
ref 7b	±16.7	±55	±55	frozen aqueous solution 77 K
ref 7a	±17.2	±48.8	±48.8	crystal, 298 K
ref 9	−18.4 (1)			crystal, 10 K
			N3H	
		H8	H6	
ref 9	−2.0	−1.6	−13.5	crystal, 10 K

planar arrangement corresponds to a first-order saddle point, about 2 kJ/mol higher in energy.

The normal mode that corresponds to C6 inversion in the 6-yl radical is well-separated and has a sufficiently low harmonic frequency to require an anharmonic treatment. Thus, the vibrational levels supported by motion along the LSP defined by the two energy minimums were computed following the procedure described in the computational details. The wave functions corresponding to the lowest vibrational levels are shown in Figure 2. The low barrier makes possible a strong coupling between the vibrational states of the two wells so that, already, the lowest level is delocalized. It must be noticed that such a small energy barrier between the two isomers could be significantly affected by either crystal constraints or by other environmental effects. As a consequence, the 6-yl radical might have an average planar geometry, depending upon the experimental conditions (e.g., temperature). Figure 3 shows the evolution of hyperfine splittings connected to the out-of-plane displacement of the C6 atom along the LSP.

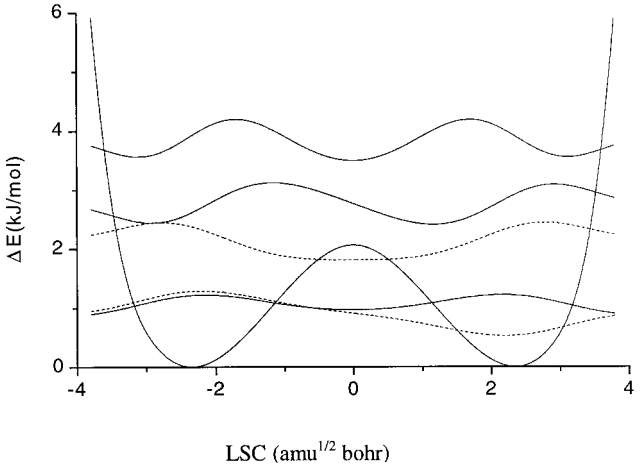

Figure 2. Potential energy and lower vibrational level for ring puckering of 6-yl.

It is quite apparent that the splittings of the considered hydrogens (H^α and H^β) are significantly affected by this deformation. Our best estimate for H^β, taking into account vibrational averaging (37.2 G), is close to the experimental value in frozen aqueous solution (±40 G)[7b] and in the crystal (±37.5 G).[7a] An even better agreement is found for the hcc of H^α, whose experimental value (±18.6 G) is nearly identical to our best estimate (−18.5 G).

To the best of our knowledge, there is only one set of experimental data available for the N3H radical, which includes three hydrogen hcc's. The first hcc is 13.5 G and has been assigned to H6, because it is characteristic of an interaction between unpaired π-electron spin density and a $CH^\bullet$ fragment, but the second arises from a π-NH interaction (−2.0 G). Our

Table 3. Hyperfine Coupling Constants (G), Computed at the UB3LYP Level[a,b]

	N3H					6-yl					5-yl				
atom	ref 21[c]	EPR−II[d]	EPR−II	EPR−III	PCM[e]	ref 21[c]	EPR−II[d]	EPR−II	EPR−III	PCM[e]	ref 21[c]	EPR−II[d]	EPR−II	EPR−III	PCM[e]
Hα	0.6	0.6 (−3.1)	0.2	−0.6	0.0	−14.2	−15.0 (−15.1)	−15.0	−15.6	−15.6	−16.3	−17.9 (−17.1)	−17.4	−18.2	−17.9
Hβ						14.0	14.5 (37.7)	14.6	15.0	16.1	45.1	49.1 (45.8)	51.3	52.1	54.7
Hβ′						44.6	47.8 (38.0)	48.0	48.0	50.7	42.0	47.0 (44.5)	50.1	51.6	47.5
H4	19.6	21.9 (−3.0)	21.0	18.0	20.2										
H4′	−1.1	−1.0 (−2.8)	−1.1	−1.0	−1.2										
H3	−13.7	−15.6 (−16.5)	−15.5	−15.8	−15.7										
H1	−3.0	−3.4 (−3.0)	−3.1	−3.4	−3.2										

[a] Using the UB3LYP/6-311G(d,p) geometries, unless otherwise noted. [b] Values in parentheses are reported for the planar conformations. [c] B3LYP/6-31G(d) geometry, PW86/6-311G(2d,p) hyperfine couplings. [d] B3LYP/6-31G(d) geometry. [e] EPR-II basis set.

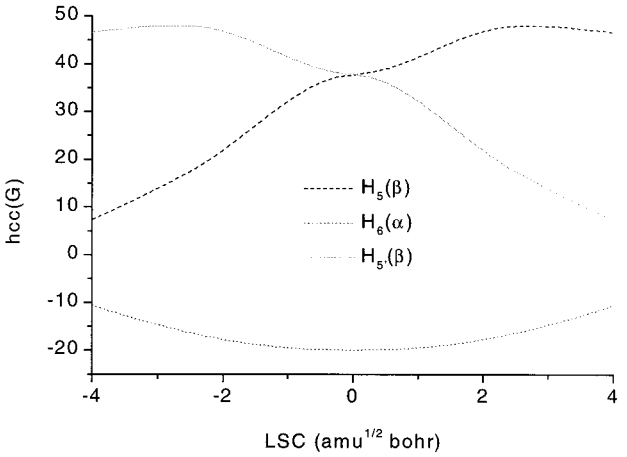

Figure 3. Variation of isotropic hcc's as a function of the ring puckering of 6-yl.

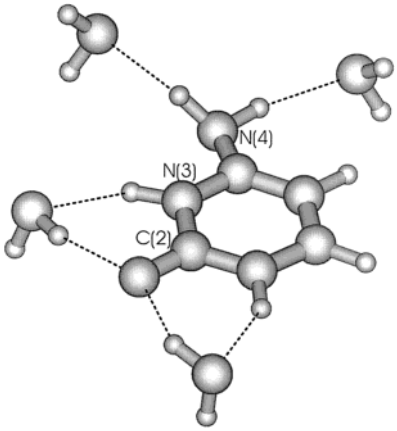

Figure 4. Schematic drawing of an adduct between N3H and four water molecules.

computations in the gas phase slightly underestimate both values, giving −15.6 and −2.0 G, respectively, at the B3LYP/EPR-II level for the puckered equilibrium structure. The third experimental hcc is quite small (−1.6 G) and has been assigned to H4 atoms. In this case, because of the nonplanar arrangement of the minimum energy structure, we found two nonequivalent hydrogens, one at 21.9 G and the other at −1.0 G. On the other hand, in the completely planar structure, both hydrogen atoms have small hcc's (−2.8 and 3.0 G), whereas the hcc's of the other hydrogens remain essentially unmodified. The effect of extending the basis set from EPR-II to EPR-III is always quite small (max, 1.5 G): however, it improves the agreement with the experiments.

The hcc's of the H4 atoms might be affected by two different large-amplitude modes, namely the out-of-plane bending of the NH_2 group and the rotation along the C4−N4 bond. In a previous study of the anilino radical,[30] we showed that the computed hcc's are insensitive to vibrational averaging from the out-of-plane motion of the radical center, so the LSP for the N3H radical was traced, considering as the DC the rotation of the NH group around the C4N4 bond. Although this motion modifies the hcc's of H4 atoms, the torsional barrier is sufficiently high to prevent any significant vibrational averaging effect (see Table 4). As a result, we are left with the only possibility being that environmental effects not taken into account explicitly by our model (e.g., specific intermolecular hydrogen bonds) induce a shift from a pyramidal to a planar or nearly planar amino group. To investigate this aspect in further detail, we have considered the supermolecule formed by the NH3 radical and four water molecules. One representative minimum energy structure is shown in Figure 4.

Table 4. Different Contributions (G) to the Hyperfine Coupling Constants[a]

	static	Δ(basis)	Δ(envir)	Δ(vib)	best est[b]	exp[b,c]
6-yl						
H^{α}	−15.0	−0.6	−0.6	−2.3	−18.5	±18.6
H^{β}	14.6	+0.4	+1.5	+21.2	37.7	±40
H^{β}	48.0	+0.0	+2.7	−13.0	37.7	±40
5-yl						
H^{α}	−17.4	−0.8	−0.5	+0.2	−18.5	±16.7
H^{β}	51.3	+0.8	+3.4	−3.4	52.1	±55
H^{β}	50.1	+1.5	−2.6	+3.1	52.1	±55
N3H						
H^{α}	0.2	−0.8	−0.2	0.1	−0.7	−2.0
H4	21.0	−3.0	−0.8	−0.5	16.7	−1.6
H4′	−1.1	+0.1	−0.1	0.1	−1.0	−1.6
H6	−15.5	−0.3	−0.1	0.2	−15.7	−13.5
H1	−3.1	−0.3	−0.1	−0.1	−3.6	

[a] Computed at the UB3LYP level. [b] At $T = 77$ K. [c] From ref 7b, except N3H from ref 9.

The average value of H4 hcc's computed for this structure is 3 G, as compared with a value of 8 G obtained including solvent effects by the PCM. Note that the reduction of the hcc is only partially due to a less pyramidal equilibrium structure, because the electron polarization issuing from H bond formation plays a significant role. Although our results are not quantitatively accurate (intermolecular interactions in the crystal can be quite different from those between N3H and water molecules), they show, in our opinion, that modeling of environmental effects by mixed discrete-continuum models reduces the discrepancy with experiment to a limit that allows a meaningful selection between different possible structural interpretations.

Conclusions

In the present study, we have performed a comprehensive analysis of the structure and EPR features of three important radicals obtained by the addition of a hydrogen atom to cytosine.

We have shown unambiguously that the 5,6-dihydrocytos-5yl radical is effectively planar, and the 5,6-dihydrocytos-6yl radical adopts a half-chair conformation at low temperature. The planar conformation of the 5-yl radical implies the equivalence of the two β-hydrogens of the methylene group. For the 6-yl radical, two equivalent energy minimums are found, separated by a low energy barrier. In such a case, temperature effects can be sufficient to modify the values of the β-hydrogen coupling, giving rise to the values observed experimentally. Finally, proper consideration of environmental effects brings the hcc's of the N3H radical into fair agreement with experiments.

Together with the specific interest for the free radicals studied in the present work, we suggest that this kind of integrated computational approach could provide powerful additional tools for the microscopic interpretation of experimental results, especially when only partial data are available or concurrent interpretations are possible.

JA004284Z